Thermochimica Acta 487 (2009) 74–79

Contents lists available at ScienceDirect

Thermochimica Acta

journal homepage: www.elsevier.com/locate/tca

Synergistic effect of iron and intumescent flame retardant on shape-stabilized phase change material

Ping Zhang[a], Yuan Hu[a,*], Lei Song[a], Hongdian Lu[a,c], Jian Wang[a], Qingqing Liu[a,b]

[a] *State Key Laboratory of Fire Science, University of Science and Technology of China, 96 Jinzai Road, Hefei, Anhui 230026, PR China*
[b] *Department of Polymer Science and Engineering, University of Science and Technology of China, 96 Jinzai Road, Hefei, Anhui 230026, PR China*
[c] *Department of Chemical and Materials Engineering, Key Laboratory of Powder and Energy Materials, Hefei University, Hefei, Anhui, 230022, PR China*

ARTICLE INFO

Article history:
Received 7 November 2008
Received in revised form
26 December 2008
Accepted 8 January 2009
Available online 20 January 2009

Keywords:
Phase change material (PCM)
Iron
Intumescent flame retardant (IFR)
Synergistic effect
Paraffin

ABSTRACT

This paper deals with the preparation of paraffin/high density polyethylene (HDPE)/intumescent flame retardant (IFR)/iron as flame retardant shape-stabilized phase change material (FSPCM). The influences of iron for FSPCM on morphology, flammability property, latent heat and thermal conductive property were characterized by scanning electron microscopy (SEM), cone calorimeter, differential scanning calorimetry (DSC) and hot disk thermal constants analyser. It was found that iron could be well dispersed into the composite formed by HDPE and paraffin; the flame retardant efficiency of IFR could be improved by adding iron; the thermal conductivity of FSPCM could be increased due to the high thermal conductivity of iron. At the same time, the possible flame retardant mechanism for paraffin/HDPE/IFR with iron as a FSPCM was proposed.

© 2009 Elsevier B.V. All rights reserved.

1. Introduction

In recent years, phase change materials have been applied in many fields such as solar heating system, peak shift of electrical demands and building energy conservation [1–3]. Different inorganic and organic substances are employed for the phase change materials such as salt hydrates, salts, metals, alloys, paraffin, fatty acids/esters and polyalcohol. Among the investigated phase change materials, paraffin exhibits desirable properties, such as high heat of fusion, little or no supercooling, self nucleating behavior, thermal and chemical stability. However, it presents a low thermal conductivity. This property reduces the rates of heat storage and release during melting and solidification cycles. Different techniques to improve this low thermal conductivity have been studied, such as adding expanded graphite, carbon fiber, aluminum and copper in the PCM [4–7].

Recently, a new type phase change material called shape-stabilized phase change material composed of phase change material and supporting material is developed. Different phase change materials should have congruent supporting materials. Just as the phase change material bases on paraffin, supporting material should have a similar skeleton, such as HDPE, PP, SBS, etc. [8–10], paraffin can be dispersed easily into the polymer network formed by the supporting material. As long as the operating temperature is below the melting point of the supporting material, the shape-stabilized PCM can keep its shape even when the paraffin changes from solid to liquid. However, due to the chemical constitutions of paraffin and supporting materials, the shape-stabilized PCM is easily flammable.

The objective of this study is to investigate a flame retardant shape-stabilized phase change material (FSPCM) with a good thermal conductivity. We study the addition of intumescent flame retardant (IFR) and iron into the HDPE/paraffin composite. The results show that synergistic effect between iron and IFR (containing ammonium polyphosphate (APP), pentaerythritol (PER) and melamine (MA)) was observed in the composite. At the same time, the microstructures, flame retardant properties, ingredients of the char residues, latent heat and thermal conductivity properties have been studied by means of scanning electron microscopy (SEM), cone calorimeter, differential scanning calorimetry (DSC) and hot disk thermal constants analyser.

2. Experiments

2.1. Materials

HDPE was obtained from Daqing Petrochemical Company, China Petroleum; Paraffin (latent heat 142.61 J/g) was used as phase

---

[*] Corresponding author. Fax: +86 551 3601664.
E-mail address: yuanhu@ustc.edu.cn (Y. Hu).

0040-6031/$ – see front matter © 2009 Elsevier B.V. All rights reserved.
doi:10.1016/j.tca.2009.01.006

Table 1
The compositions of the FSPCMs.

Sample	Paraffin/HDPE/IFR (3:1:1)	Iron (phr)
FSPCM1	100	0
FSPCM2	100	1
FSPCM3	100	3
FSPCM4	100	5
FSPCM5	100	10

change material; APP and PER (powder, average size <10 μm) were provided by Keyan Company; MA was supplied by Sinopharm Chemical Ltd. (Shanghai, China); Iron (powder) was obtained from Tianjin Da-mao Chemistry Company.

2.2. Preparation of FSPCMs

The samples are listed in Table 1. The blends were premixed in a high-speed blender, and then extruded by a twin-screw extruder (TE-35, KeYa, China), the temperature range of the twin-screw extruder was 90–160 °C and screw speed was 250 rpm, thus the FSPCMs were obtained.

2.3. Characterization

SEM observations were studied to observe their cracking surfaces for FSPCMs and the char residues of FSPCMs after the cone calorimeter tests. SEM images were taken with a PHILIPS XL30ESEM microscope.

The flammability property was characterized by the cone calorimeter (Stanton Redcroft, UK). All samples ($100 \times 100 \times 3\,\mathrm{mm}^3$), which were studied according to ISO 5660 standard procedures, were wrapped in aluminium foil and exposed horizontally to an external heat flux of 35 kW/m^2 and the results were reproducible to within ±10%.

DSC was used to study the latent heat, phase change temperatures and thermal cycling of the FSPCMs, which were carried out in argon atmosphere by means of the DT-50 thermal analyzer from 20 °C to 170 °C at heating rate of 10 °C/min and a flow rate of 30 ml/min. A small quantity of sample (usually from 7 mg to 10 mg) was sealed in a small aluminum pan. The precisions on the calorimeter and temperature measurements were ±2.0% and ±2.0 °C, respectively. Thermal cycling was studied within five cycles started from −20 °C to 80 °C. The samples were equilibrated at −20 °C and 80 °C for 3 min, with heating and cooling rates of all 10 °C/min.

The thermal conductive properties are characterized by Hot Disk Thermal Constants Analyser 2500. A constant voltage was applied for 40 s and the temperature raise by circulating current along the platinum wire was recorded by a thermocouple. The measurements were repeated three times for each sample in order to minimize the error. The precision on thermal conductivity was ±2.0%.

3. Results and discussion

3.1. Microstructures of the FSPCMs

Fig. 1(a) shows that paraffin is dispersed into the network formed by HDPE used as the supporting material. This dispersion provides a mechanical strength to the whole compound. There-

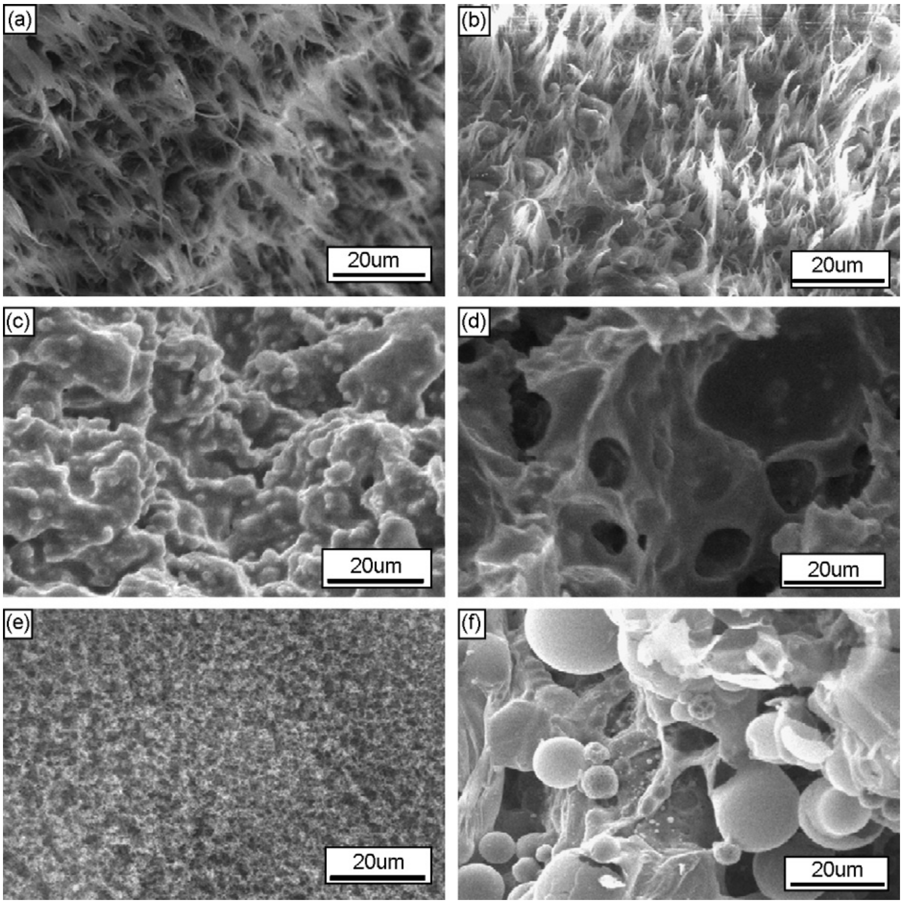

Fig. 1. The SEM photographs of FSPCM: (a) FSPCM1, (b) FSPCM3; the char residues: (c) the surface of FSPCM1, (d) the inner of FSPCM1, (e) the surface of FSPCM3, (f) the inner of FSPCM3.

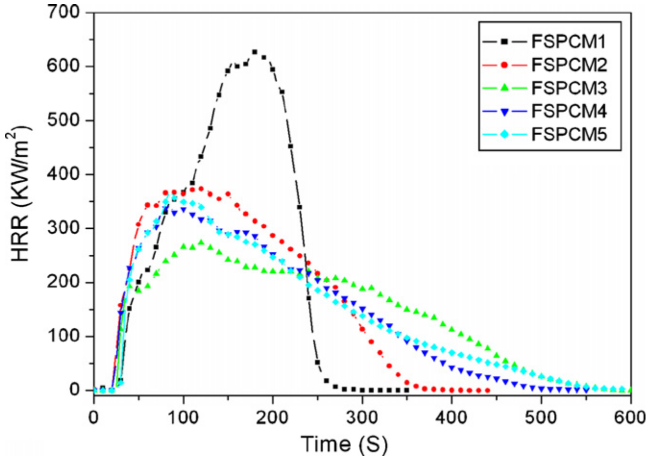

Fig. 2. Heat release rate (HRR) of the FSPCMs.

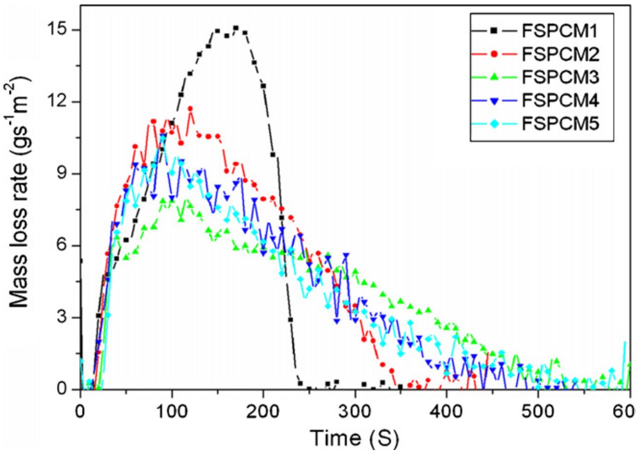

Fig. 3. Mass loss rate (MLR) of the FSPCMs.

fore, the material can maintain its shape in the solid state without seepage of the melted paraffin. Fig. 1(b) indicates that iron is well dispersed in the composite; also this structure could protect iron from oxidization.

3.2. *Flammability properties*

The cone calorimeter is one of the most effective bench-scale methods for studying the flammability properties of materials. Cone calorimeter results have been found to correlate well with those obtained from large-scale fire tests and can be used to predict the behaviour of materials in real fires [11]. The heat release rate (HRR), especially peak HRR, has been found to be the most important parameter to evaluate fire safety. Fig. 2 and Table 2 show the effects of iron on the HRRs of paraffin/HDPE/IFR composites within 10phr loading level. It can be found that when iron is introduced into paraffin/HDPE/IFR composites, the times to combustion are mostly prolonged to 338–553 s from 214 s, while the peak HRR decreased greatly, which indicates that iron decelerates the decomposition rate at the first stage and helps the composites to form more efficient char layer to protect material from further combustion. The cone calorimeter data of the FSPCMs are listed in Table 2. It can be found that the peak HRR value is decreased by increasing the loading of iron up to 3phr iron, then decrease on the contrary. The peak HRR values of FSPCMs are decreased by 40.22% (FSPCM2), 56.32% (FSPCM3), 45.46% (FSPCM4) and 40.98% (FSPCM5) in comparison with that of FSPCM1. The total heat release (THR) of FSPCMs are lower than that of without iron, and the THR/total mass loss has the same tide with the average HRR. It means that the addition of iron into the composite could induce the decrease of the heat generated. It knows that the HRR is a function of heat generation rate and heat transfer, and the heat generation rate is related with oxygen transfer during the combustion, so the decrease of HRR is mostly owing to the decrease of its transfer rate. In other words, the addition of iron into the paraffin/HDPE/IFR composites could improve the barrier property of the char layer, and thus the transfer rate is retarded.

Another primary parameter which is relevant to HRR of the FSPCMs is the mass loss rate (MLR) during combustion. Fig. 3 shows that the trend of the evolution of the MLR is significantly reduced from the values observed for the FSPCM1, which has the homologous phenomenon with the HRR in the cone calorimeter.

In order to investigate the flame retardant mechanism, the char residues of the FSPCMs after the cone calorimeter test are studied by SEM. Fig. 1(c)–(f)) shows the SEM photographs of surface and inner char layers of the FSPCM1 and FSPCM3, respectively. It can be seen that the surface of the FSPCM3 (Fig. 1(e)) is more compact than that of FSPCM1 (Fig. 1(c)). The inner structures of chars obtained from FSPCM1 and FSPCM3 are shown in Fig. 1(d) and (f), respectively. The two chars show irregular swollen structures, the swollen structure of FSPCM1 is constituted of broken cells, but the cells of the inner char layer for FSPCM3 are closed. These results can be approved that the presence of iron improves the stability of the char layer. The closed structural cells improve the thermal protection properties of char layer, which is in good agreement with the cone results.

On the basis of cone calorimeter results, the possible mechanism for the synergism of iron with paraffin/HDPE/IFR system was concluded. First the APP and MA release water and ammonia at the beginning of heating, polyphosphoric acid produced by the elimination of ammonia from APP could attack hydroxyl bonds of PER with formation of phosphoric ester. The phosphoric ester is thermally decomposed at higher temperatures, leading to formation of three-dimensional network structures. At the same time, the C–H bonds for paraffin and HDPE are dehydrogenated and oxidized with formation of C–O–OH groups on the backbone. Then the crosslinking occurs between paraffin and IFR or HDPE and IFR, and a complicated network could be formed [12,13]. Another reaction taking place is the iron is introduced into paraffin/HDPE/IFR system. The reaction can occur in two ways. During heating, iron could promote the release of ammonia and water from MA and APP, and form Fe^{n+} due to multiple valency of Fe. Also APP could react with Fe^{n+} which takes as bridges, the formation would bring about a stabilization of the APP and increase the molecular weight, which could increase the viscosity of the melt during pyrolysis and combustion.

Table 2
Data recorded in cone calorimeter experiments for all samples.

Sample	Time to ignition (s)	Flame out	THR (MJ/m^2)	THR/mass lost (MJ/m^2 g)	Peak HRR (kW/m^2)	Average HRR (kW/m^{2}s)
PCM1	27	241	90.4	4.09	627.35	368.42
PCM2	28	366	81.9	3.50	375.25	238.63
PCM3	30	583	83.7	3.78	274.03	150.39
PCM4	27	496	82.2	3.65	341.53	173.64
PCM5	30	527	83.8	3.84	370.28	168.35

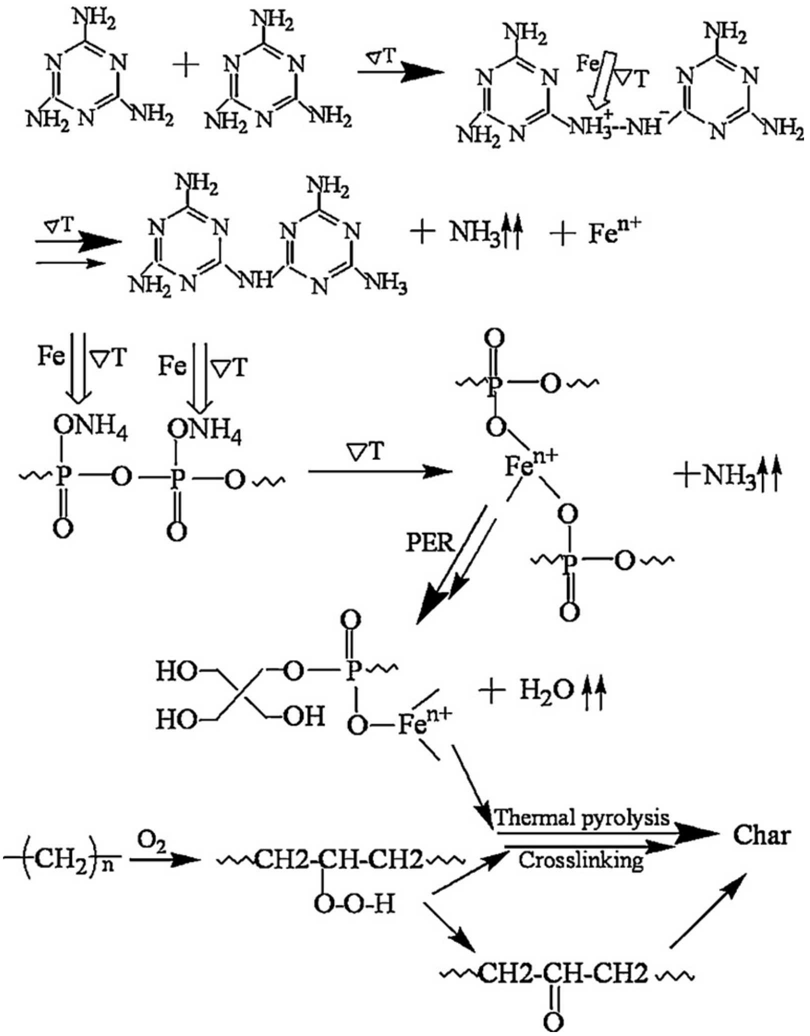

Scheme 1. Possible reaction mechanisms of char formation during the combustion of paraffin/HDPE/IFR system with iron.

Above all reasons, it could be explained that iron could improve the thermal stability of the paraffin/HDPE/IFR phase change material. Especially, when increasing the mass of the iron, the negative effect could exceed the positive effect on the fire properties, due to reducing the content of IFR. The scheme of the combustion mechanism for paraffin/HDPE/IFR system with iron is shown in Scheme 1.

3.3. Thermal properties of the FSPCMs

Thermal properties of the prepared FSPCMs, such as phase transition temperature, melting temperature and latent heat, are determined by a DSC thermal analyzer. The thermograms of the paraffin, HDPE and the FSPCMs are showed in Figs. 4 and 5. DSC curves present data to evaluate the latent heat values which are presented in Table 3. The typical DSC curve of the pure paraffin used as phase change material shows in Fig. 4, it can be seen that there are two peaks in the DSC curve of the pure paraffin. The sharp peek represents the solid–liquid phase change of the paraffin (melting temperature $T_m = 55.36\,^\circ C$), and the minor peak is associated with the solid–solid phase transition of paraffin (transition temperature $T_t = 37.93\,^\circ C$). Fig. 5 shows that the phase change peaks of the paraf-

Table 3
Latent heat of the paraffin and FSPCMs.

Samples	Latent heat (J/g)
Paraffin	142.6
FSPCM1	79.91
FSPCM2	76.57
FSPCM3	71.15
FSPCM4	70.31
FSPCM5	68.73

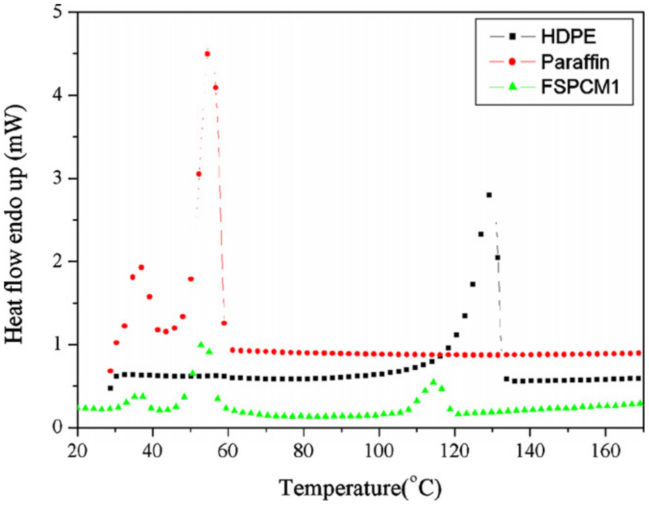

Fig. 4. The DSC curves of paraffin, HDPE and FSPCM1.

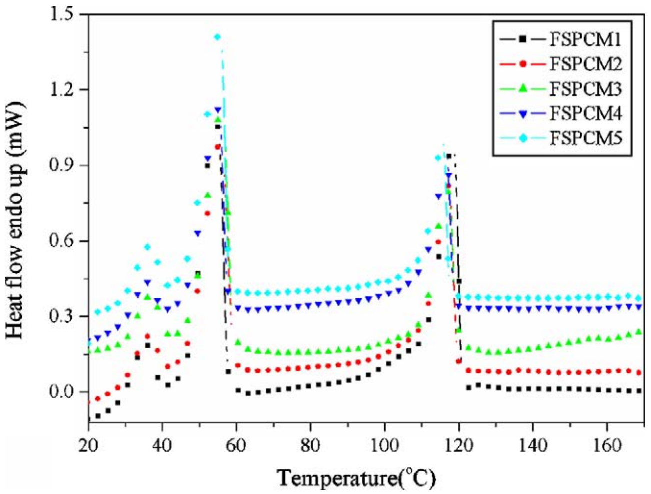

Fig. 5. The DSC curves of the FSPCMs.

fin and HDPE are still existence in the FSPCMs, and the thermal characteristics of the FSPCMs are very close to those of the pure paraffin and HDPE, this is because there is no chemical reaction between the paraffin and HDPE in the FSPCMs. However, the total latent heats (listed in Table 3) of the FSPCMs are lower than theoretically calculated values by multiplying the latent heat of the dispersed paraffin with its weight percentage. The result could be explained that the higher content of HDPE in PCM formed more intense network structure and molecular heat movement of paraffin was confined more excessive.

DSC is also used to investigate the changes of latent values under conditions of thermal cycling with the temperature from −20 °C to 80 °C. For the test, the FSPCM1 and FSPCM3 are chosen. The energy storage or release capacities of the FSPCMs are measured during thermal cycles, the typical DSC curves and results are showed in Figs. 6 and 7 and Table 4. It can be seen that the effect of thermal cycle number on thermal stability of the FSPCMs with respect to the changes in its thermal properties can be evaluated. The FSPCMs with and without iron all have good thermal reliability in terms of the changes in phase change temperatures.

3.4. The thermal conductivities of the FSPCMs

The thermal conductivities of the FSPCMs are measured using the previously mentioned apparatus. Thermal conductivities (K) of the prepared samples are calculated based on transient hot-wire method [14] using

$$k = \left(\frac{VI}{4\pi L}\right) / \left(\frac{\mathrm{d}T}{\ln t}\right)$$

when a material has a better thermal conductivity, its temperature change speed would be higher than others in the same condition, the temperature rising curve of the FSPCM would be gentler and it would appear at neither side. The temperature changes of the FSPCM1-3 are depicted in Fig. 8. The thermal conductivities of FSPCM2 (0.38 W/mK) and FSPCM3 (0.42 W/mK) increase as 5.56% and 16.67% in comparison with that of FSPCM1 (0.36 W/mK), respectively. This is attributed to high thermal conductivity of the iron. When iron is introduced into the paraffin/HDPE/IFR system, the iron could form a more effective thermal conductive network. The more iron is added, the better thermal conductivity for FSPCM can be obtained.

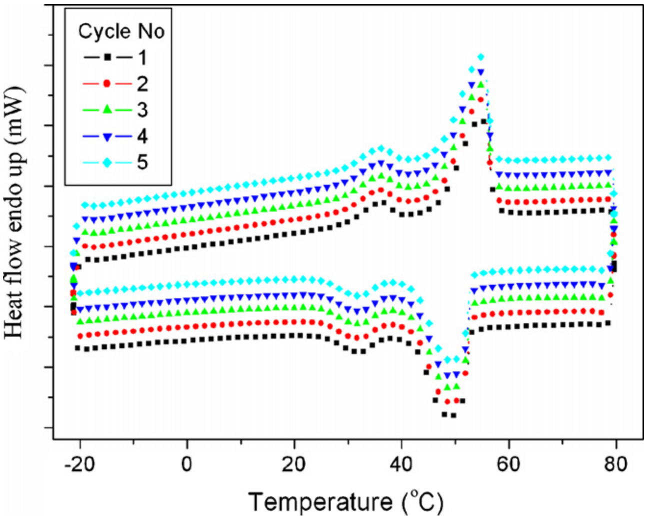

Fig. 6. The DSC curves change during thermal cycling of FSPCM1.

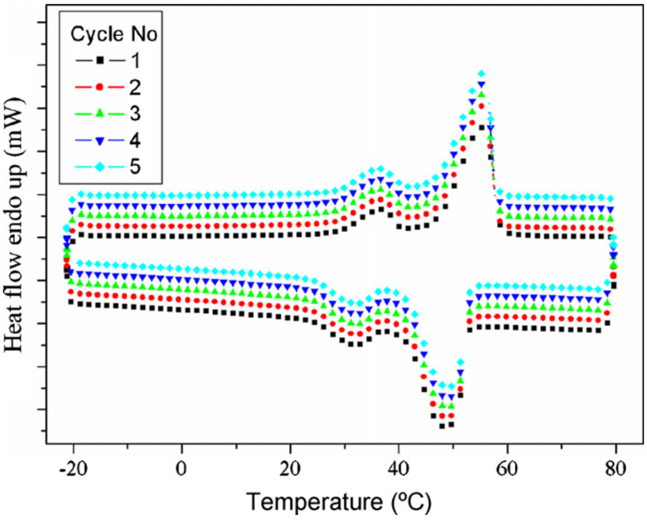

Fig. 7. The DSC curves change during thermal cycling of FSPCM3.

Table 4
DSC data of FSPCM1 and FSPCM3 during thermal cycling.

Sample	Cycle no.	Energy storage capacity (J/g)	Energy release capacity (J/g)	Sample	Cycle no	Energy storage capacity (J/g)	Energy release capacity (J/g)
FSPCM1	1	78.41	80.67	FSPCM3	1	70.65	72.49
	2	78.41	80.87		2	72.43	72.91
	3	79.88	81.38		3	72.70	72.92
	4	79.41	80.99		4	72.86	73.04
	5	79.96	81.13		5	72.54	72.71

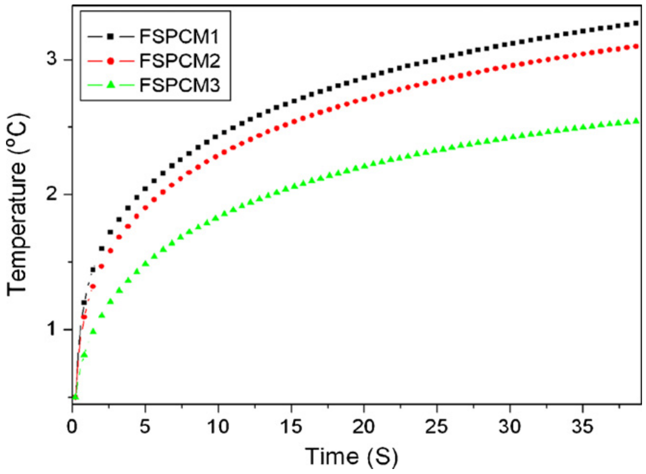

Fig. 8. Temperature changes of the FSPCM1, FSPCM2 and FSPCM3.

4. Conclusions

Flame retardant shape-stabilized phase change materials based on HDPE, paraffin, IFR and iron are studied in this paper. The SEM images show that paraffin is dispersed into the network formed by HDPE, and iron can be well dispersed in the FSPCMs. When iron is introduced into paraffin/HDPE/IFR system, the flame retardance of FSPCMs can be improved because the synergistic effect between iron and IFR was observed. The latent heats of the FSPCMs found on the mass fraction of paraffin, but they are lower than theoretically calculated values, also the FSPCMs with and without iron all have good thermal reliability in terms of the changes in phase change temperatures. The thermal conductivity of FSPCMs can be improved owing to more effective thermal conductive network formed by iron.

Acknowledgements

The work was financially supported by the National Key Technology R&D Program (2006BAK06B06, 2006BAK06B07, 2006BAK01B03), China Postdoctoral Science Foundation (20080430101), and Program for New Century Excellent Talents in University.

References

[1] M. Kenisarin, K. Mahkamov, Renew Sust. Energy Rev. 11 (2007) 1913.
[2] M.M. Farid, A.M. Khudhair, S.A.K. Razack, et al., Energy Convers. Manage. 45 (2004) 1597.
[3] V.V. Tyagi, D. Buddhi, Renew Sust. Energy Rev. 11 (2007) 1146.
[4] A. Sari, A. Karaipekli, Appl. Therm. Eng. 22 (2007) 1271.
[5] A. Karaipekli, A. Sari, K. Kaygusuz, Renew Energy 32 (2007) 2201.
[6] E-B.S. Mettawee, G.M.R. Assassa, Sol Energy 81 (2007) 839.
[7] L.F. Cabeza, H. Mehling, S. Hiebler, et al., Appl. Therm. Eng. 22 (2002) 1141.
[8] H. Hong, X. Ge, Sol. Energy Mater. Sol. Cells 64 (2000) 37.
[9] I. Krupa, G. Mikova, A.S. Luyt, Eur. Polym. J. 43 (2007) 895.
[10] M. Xiao, B. Feng, K. Gong, Energy Convers. Manage. 43 (2002) 103.
[11] Z.Z. Wang, B.J. Qu, W.C. Fang, P. Huang, J. Appl. Polym. Sci. 81 (2001) 206.
[12] Y. Tang, Y. Hu, L. Song, R.W. Zong, Z. Gui, W.C. Fan, Polym. Degrad. Stab. 91 (2006) 234.
[13] B.K. Kandola, A.R. Horricks, Polym. Degrad. Stab. 54 (1996) 289.
[14] F. Frusteri, V. Leonardi, S. Vasta, G. Restuccia, Appl. Therm. Eng. 25 (2005) 1623.